J. Chem. Eng. Data **2010,** *55,* 1580–1587

Phase Behavior, Densities, and Isothermal Compressibility of (Carbon Dioxide + Dimethyl Carbonate)

Yucui Hou,[†,‡] Xiaoting Chen,[‡] Shuhang Ren,[‡] Zhangzuo Song,[‡] and Weize Wu*[,‡]

Department of Chemistry, Taiyuan Normal University, Taiyuan 030012, China, and State Key Laboratory of Chemical Resource Engineering, Beijing University of Chemical Technology, Beijing 100029, China

---

The phase behavior and critical parameters of ($CO_2 + CH_3CO_3CH_3$) have been determined using a high-pressure, variable-volume view cell, and their densities have also been measured in sub- or supercritical regions. The isothermal compressibility, K_T, was calculated from the density of the binary mixtures. The transition points, bubble point, dew point, and critical point, have been measured with concentrations of dimethyl carbonate from mole fractions of (0.0242 to 0.1484), temperatures from (308.15 to 337.45) K, and pressures from (6.16 to 16.67) MPa. It is demonstrated that the density and K_T are sensitive to the pressure as the pressure gets close to the critical point of the binary mixtures. K_T also increases sharply when the pressure approaches the dew points or bubble points at other compositions near the critical composition. When the pressure is much higher than the phase transition pressure or the composition is far from the critical composition, K_T is rather small, and the effect of pressure on K_T is fairly limited. The phase boundary data of the binary mixtures can be correlated well by the Peng−Robinson equation of state (PR EoS) with two binary parameters.

Introduction

Dimethyl carbonate (DMC) is a versatile compound that represents an attractive, nontoxic, and environmentally friendly alternative (1) to substitute phosgene in the synthesis of polycarbonates and iso-cyanates and (2) to replace phosgene in carbonylation reactions or dimethyl sulfate and methyl halide in methylation and alquilation reactions.[1−3] In addition, because of its high octane number and miscibility with hydrocarbons, DMC is an excellent additive for fuels, replacing methyl *tert*-butyl ether (MTBE).[4] Currently, DMC is produced mainly by the phosgene route and catalytic oxidative carbonylation of methanol.[5] Other ways to synthesize DMC were also developed, such as transesterification between cyclic carbonate and methanol, urea methanolysis, and the direct carbonation of methanol. Because of the use of highly toxic chemicals or ineffectiveness in the present ways, an environmentally benign solvent, supercritical carbon dioxide ($scCO_2$), has been employed as a solvent to reduce the problems, especially for the direct carbonation of methanol.[6−9]

Phase behavior is of great importance for many chemical processes and separations that are conducted at high pressures and high temperatures, especially for supercritical fluid processes, where phase behavior can significantly influence the reaction rate, selectivity, mass transfer properties, and so forth.[10−12] Hou et al.[13] studied the synthesis of DMC using carbon dioxide (CO_2) and methanol and found that the phase behavior affected the equilibrium conversion of methanol significantly and the conversion reached a maximum in the critical regions of the reaction system. The phase behavior for the direct synthesis of DMC from CO_2 and methanol at supercritical or near critical conditions had been measured and modeled by Piňero et al.[14] They measured the phase equilibria of CO_2 and DMC at (310, 320, and 330) K. Camy et al.[15] also

Table 1. Pure Component Parameters and Binary Parameters Used in the PR EoS and the Average Absolute Relative Deviation (AARD) for the CO_2 + DMC System

components	T_C/K	P_C/MPa	ω	k_{12}	l_{12}	AARD/%
DMC	557.0[a]	4.80[a]	0.337[a]	0.001	−0.068	2.3
CO_2	304.3[b]	7.38[b]	0.225[b]			

[a] Reported by Poling et al.[25] [b] From NIST.

Table 2. Experimental Bubble Points, Critical Points, and Dew Points of the CO_2(1) + DMC (2) Binary Mixtures at Fixed Molar Compositions[a]

T/K	P/MPa	phase transition	T/K	P/MPa	phase transition
	$x_2 = 0.0242$			$x_2 = 0.0481$	
308.15	7.52	b	308.15	7.16	b
313.15	8.22	b	313.15	7.85	b
317.85	8.66	cp	318.15	8.55	b
323.15	9.02	d	323.15	9.18	b
327.95	9.15	d	327.95	9.64	cp
332.85	9.04	d	332.85	10.09	d
337.45	8.22	d	337.45	10.45	d
	$x_2 = 0.0860$			$x_2 = 0.1180$	
308.15	6.75	b	308.15	6.42	b
313.15	7.34	b	313.15	7.02	b
318.15	8.02	b	318.15	7.63	b
323.15	8.69	b	323.15	8.29	b
327.95	9.32	b	327.95	8.92	b
332.85	9.96	b	332.85	9.62	b
337.45	10.45	b	337.45	10.18	b
	$x_2 = 0.1484$				
308.15	6.16	b			
313.15	6.78	b			
318.15	7.34	b			
323.15	7.96	b			
327.95	8.54	b			
332.85	9.18	b			
337.45	9.76	b			

[a] b: bubble point; cp: critical point; d: dew point.

---

* To whom correspondence should be addressed. E-mail: wzwu@mail.buct.edu.cn. Tel./Fax: +86 10 64427603.

[†] Taiyuan Normal University.

[‡] Beijing University of Chemical Technology.

10.1021/je900691n CCC: $40.75

studied the fluid-phase equilibria of the reacting mixture of synthesis of DMC in supercritical CO_2, and they measured the phase behavior of (carbon dioxide + DMC) at (322.65, 348.15, and 373.55) K. Isothermal phase equilibria of CO_2 and DMC had been studied at temperatures from (273 to 340) K by several research groups.[16,17] Guo et al.[18] measured the critical points of the reacting mixture at temperatures from (277.7 to 469.7) K. Supercritical or near critical conditions of pressure and temperature may be needed to enhance the kinetics and the mass transfer properties.

The knowledge of density is greatly important especially in single-phase regions in the supercritical region. In the present study, we have determined the phase behaviors, critical parameters, and densities of (CO_2 + $CH_3CO_3CH_3$) binary systems at elevated pressures up to 16.7 MPa. The compressibility of the mixtures was then studied systematically in different phase regions. We also investigated the effects of phase behavior, composition, and pressure on the density and isothermal compressibility, especially in the critical region. The measured

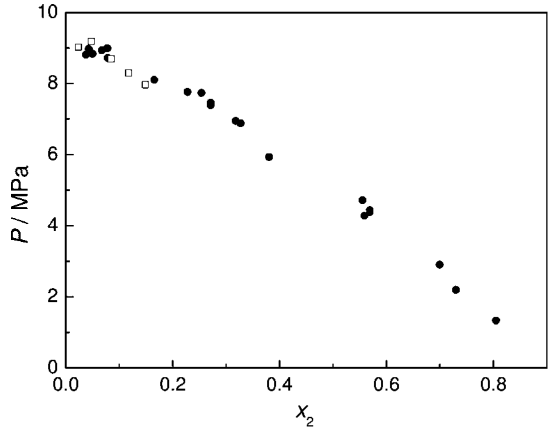

Figure 1. Phase behavior for the CO_2 (1) + DMC (2) binary mixture: ●, T = 322.65 K, by Camy et al.;[15] □, T = 323.15 K, by this work.

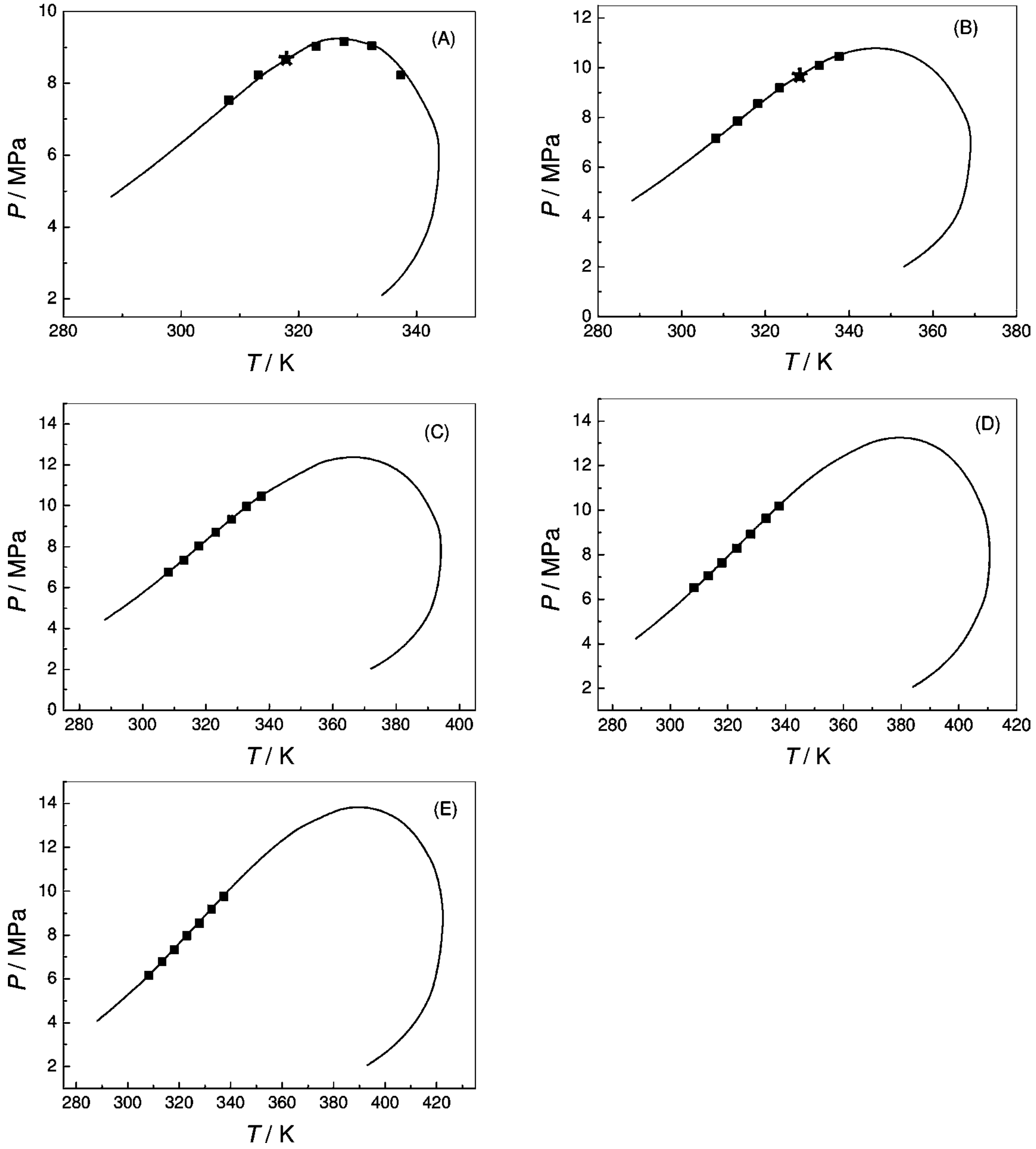

Figure 2. Phase boundary of the CO_2 (1) + DMC (2) binary mixture with different compositions: (A) x_2 = 0.0242; (B) x_2 = 0.0481; (C) x_2 = 0.0860; (D) x_2 = 0.1180; (E) x_2 = 0.1484, experimental data (in symbols); calculated results by PR-EoS (in lines); *, critical points measured).

Table 3. Densities ρ of CO_2(1) and DMC (2) Binary Mixtures under Different Conditions

P/MPa	ρ/$g \cdot cm^{-3}$	P/MPa	ρ/$g \cdot cm^{-3}$	P/MPa	ρ/$g \cdot cm^{-3}$	P/MPa	ρ/$g \cdot cm^{-3}$
T/K = 308.15		T/K = 313.15		T/K = 317.85		T/K = 323.15	
x_2 = 0.0242		x_2 = 0.0242		x_2 = 0.0242		x_2 = 0.0242	
7.52[a]	0.697[a]	8.22[a]	0.606[a]	8.66[b]	0.476[b]	9.02[c]	0.394[c]
7.63	0.705	8.25	0.613	8.71	0.485	9.08	0.401
7.78	0.718	8.29	0.622	8.72	0.490	9.12	0.408
7.99	0.731	8.38	0.636	8.75	0.498	9.17	0.417
8.23	0.744	8.49	0.650	8.78	0.506	9.23	0.427
8.48	0.755	8.59	0.665	8.82	0.517	9.28	0.436
8.87	0.770	8.76	0.681	8.88	0.529	9.35	0.447
9.18	0.780	8.92	0.692	8.93	0.542	9.41	0.458
9.64	0.792	9.11	0.705	9.00	0.555	9.48	0.470
9.92	0.799	9.42	0.721	9.07	0.569	9.55	0.482
10.18	0.806	9.63	0.731	9.15	0.583	9.62	0.495
10.60	0.814	9.96	0.744	9.25	0.599	9.71	0.509
11.01	0.822	10.28	0.755	9.35	0.611	9.80	0.523
11.29	0.828	10.58	0.765	9.50	0.628	9.90	0.536
11.75	0.836	10.98	0.775	9.71	0.646	9.93	0.541
12.02	0.839	11.40	0.785	9.91	0.663		
12.42	0.846	11.74	0.793				
12.78	0.852	12.08	0.801				
		12.52	0.809				
		12.90	0.816				
		13.27	0.823				
		13.64	0.828				
		13.96	0.833				
		14.14	0.836				
		14.56	0.842				
		14.95	0.847				
		15.23	0.851				
T/K = 327.95		T/K = 332.85		T/K = 337.45		T/K = 308.15	
x_2 = 0.0242		x_2 = 0.0242		x_2 = 0.0242		x_2 = 0.0481	
9.15[c]	0.333[c]	9.04[c]	0.282[c]	8.22[c]	0.212[c]	7.16[a]	0.787[a]
9.18	0.337	9.11	0.287	8.34	0.217	7.62	0.800
9.25	0.344	9.20	0.292	8.44	0.222	8.23	0.816
9.32	0.352	9.27	0.298	8.53	0.226	8.74	0.827
9.40	0.359	9.35	0.305	8.64	0.231	9.25	0.837
9.47	0.369	9.43	0.311	8.73	0.236	9.69	0.844
9.54	0.378	9.52	0.318	8.82	0.242	10.12	0.852
9.62	0.387	9.64	0.329	8.92	0.247	10.53	0.858
9.69	0.397	9.72	0.336	9.03	0.253	11.08	0.865
9.77	0.407	9.81	0.344	9.13	0.259	11.50	0.871
9.86	0.418	9.91	0.353	9.24	0.266	12.04	0.878
9.95	0.430	10.01	0.362	9.35	0.272	12.53	0.883
10.04	0.442	10.11	0.371	9.46	0.279	12.97	0.888
10.12	0.453	10.20	0.381	9.57	0.287	13.66	0.895
		10.30	0.391	9.69	0.295	14.46	0.903
		10.38	0.399	9.81	0.304	15.24	0.911
		10.49	0.410	9.93	0.311		
		10.58	0.417				
T/K = 313.15		T/K = 318.15		T/K = 323.15		T/K = 328.15	
x_2 = 0.0481		x_2 = 0.0481		x_2 = 0.0481		x_2 = 0.0481	
7.85[a]	0.740[a]	8.55[a]	0.683[a]	9.18[a]	0.607[a]	9.64[b]	0.532[b]
8.05	0.748	8.70	0.693	9.26	0.617	9.71	0.543
8.26	0.757	8.88	0.706	9.41	0.638	9.80	0.556
8.51	0.767	9.14	0.721	9.57	0.650	9.91	0.570
8.93	0.780	9.45	0.735	9.75	0.666	10.03	0.585
9.48	0.795	9.76	0.748	10.01	0.683	10.18	0.600
9.96	0.807	10.20	0.758	10.35	0.700	10.34	0.615
10.42	0.816	10.74	0.777	10.78	0.719	10.54	0.632
11.01	0.827	11.25	0.789	11.36	0.739	10.72	0.645
11.43	0.834	11.77	0.800	11.87	0.754	10.94	0.659
11.95	0.842	12.24	0.809	12.39	0.768	11.19	0.673
12.45	0.849	12.72	0.818	12.92	0.780	11.35	0.681
12.95	0.856	13.28	0.826	13.55	0.792		
13.45	0.863	13.73	0.833				
13.98	0.869	14.24	0.841				
14.62	0.877	14.71	0.847				
15.21	0.882	15.30	0.854				
15.90	0.890	16.25	0.865				
T/K = 332.85		T/K = 337.45		T/K = 308.15		T/K = 313.15	
x_2 = 0.0481		x_2 = 0.0481		x_2 = 0.0860		x_2 = 0.0860	
10.09[a]	0.484[a]	10.45[a]	0.450[a]	6.75[a]	0.864[a]	7.34[a]	0.834[a]
10.25	0.506	10.67	0.470	7.94	0.881	8.35	0.852
10.35	0.517	10.78	0.481	8.73	0.890	8.79	0.859
10.42	0.525	10.89	0.492	9.63	0.900	9.25	0.865
10.52	0.538	11.01	0.504	10.13	0.905	9.72	0.871
10.64	0.550	11.16	0.517	10.93	0.913	10.13	0.876
10.74	0.560	11.31	0.530	11.34	0.917	10.87	0.885
10.89	0.574	11.48	0.543	11.80	0.921	11.12	0.888
11.06	0.588	11.65	0.558	12.21	0.924	11.71	0.893

Table 3. Continued

P/MPa	ρ/g·cm^{-3}	P/MPa	ρ/g·cm^{-3}	P/MPa	ρ/g·cm^{-3}	P/MPa	ρ/g·cm^{-3}
11.26	0.603	11.85	0.573	12.85	0.929	12.13	0.898
11.50	0.619	12.10	0.589	13.35	0.934	12.70	0.903
11.76	0.636	12.36	0.607	13.85	0.937	13.58	0.911
11.99	0.650			14.14	0.939	14.12	0.915
12.28	0.663			14.76	0.944	14.75	0.920
12.63	0.678			15.06	0.946	15.22	0.924
				15.49	0.949	15.93	0.930
				16.01	0.953	16.40	0.933
T/K = 318.15		T/K = 323.15		T/K = 327.95		T/K = 332.85	
$x_2 = 0.0860$		$x_2 = 0.0860$		$x_2 = 0.0860$		$x_2 = 0.0860$	
8.02^{a}	0.802^{a}	8.69^{a}	0.762^{a}	9.32^{a}	0.724^{a}	9.96^{a}	0.682^{a}
8.41	0.812	8.88	0.769	9.72	0.740	10.03	0.686
8.83	0.820	9.22	0.779	9.99	0.750	10.20	0.695
9.16	0.827	9.76	0.792	10.40	0.762	10.38	0.704
9.81	0.838	10.28	0.803	10.74	0.772	10.53	0.711
10.26	0.845	10.74	0.813	11.18	0.782	10.86	0.724
10.82	0.853	11.23	0.822	11.65	0.792	11.27	0.738
11.19	0.858	11.67	0.829	12.21	0.802	11.75	0.751
11.74	0.865	12.31	0.839	12.75	0.812	12.27	0.765
12.23	0.871	12.74	0.844	13.20	0.819	12.75	0.775
12.69	0.876	13.19	0.851	13.68	0.826	13.23	0.784
13.27	0.882	13.74	0.857	14.17	0.833	13.76	0.794
13.84	0.888	14.23	0.863	14.71	0.840	14.29	0.803
14.29	0.893	14.73	0.868	15.16	0.846	14.72	0.810
14.83	0.898	15.22	0.873	15.66	0.852	15.33	0.819
15.28	0.902	15.66	0.878	16.18	0.858	15.76	0.825
15.76	0.906	16.13	0.883			16.20	0.831
16.30	0.910						
T/K = 337.45		T/K = 308.15		T/K = 313.15		T/K = 318.15	
$x_2 = 0.0860$		$x_2 = 0.1180$		$x_2 = 0.1180$		$x_2 = 0.1180$	
10.45^{a}	0.631^{a}	6.42^{a}	0.904^{a}	7.02^{a}	0.880^{a}	7.63^{a}	0.856^{a}
10.48	0.634	6.90	0.909	7.50	0.886	7.85	0.859
10.55	0.640	7.68	0.917	8.05	0.893	8.19	0.864
10.63	0.644	8.20	0.922	9.00	0.903	8.61	0.870
10.80	0.654	9.03	0.929	9.65	0.910	9.13	0.876
11.08	0.669	9.67	0.935	10.30	0.916	9.58	0.882
11.38	0.684	10.60	0.942	11.01	0.922	10.18	0.889
11.78	0.700	11.18	0.946	11.55	0.927	10.75	0.895
12.27	0.716	12.30	0.954	12.03	0.930	11.28	0.900
12.80	0.732			12.70	0.935	11.80	0.905
13.17	0.742			13.25	0.940	12.28	0.909
13.73	0.755			13.73	0.943	12.77	0.913
14.22	0.766			14.27	0.947	13.29	0.918
14.71	0.775					13.75	0.922
15.15	0.783					14.24	0.925
15.74	0.792					14.72	0.929
16.25	0.801					15.25	0.933
						15.82	0.937
						16.26	0.940
T/K = 323.15		T/K = 327.95		T/K = 332.85		T/K = 337.45	
$x_2 = 0.1180$		$x_2 = 0.1180$		$x_2 = 0.1180$		$x_2 = 0.1180$	
8.29^{a}	0.829^{a}	8.92^{a}	0.801^{a}	9.62^{a}	0.768^{a}	10.18^{a}	0.737^{a}
8.54	0.833	9.16	0.806	9.82	0.773	10.35	0.743
8.96	0.840	9.47	0.812	10.04	0.780	10.62	0.751
9.31	0.845	9.76	0.818	10.35	0.788	10.94	0.760
9.74	0.852	10.24	0.827	10.74	0.796	11.29	0.769
10.22	0.859	10.74	0.835	11.20	0.805	11.70	0.779
10.74	0.866	11.22	0.842	11.74	0.815	12.19	0.789
11.23	0.872	11.72	0.849	12.16	0.822	12.66	0.798
11.75	0.878	12.20	0.855	12.70	0.830	13.22	0.807
12.27	0.883	12.68	0.861	13.19	0.837	13.64	0.814
12.75	0.888	13.32	0.868	13.70	0.843	14.17	0.821
13.31	0.894	13.78	0.873	14.23	0.850	14.73	0.829
13.83	0.898	14.31	0.879	14.76	0.856	15.28	0.836
14.27	0.902	14.80	0.884	15.29	0.861	15.77	0.842
14.75	0.907	15.26	0.888	15.74	0.866	16.40	0.849
15.25	0.911	15.74	0.892	16.37	0.872		
15.74	0.914	16.33	0.897				
16.43	0.920						
T/K = 308.15		T/K = 313.15		T/K = 318.15		T/K = 323.15	
$x_2 = 0.1484$		$x_2 = 0.1484$		$x_2 = 0.1484$		$x_2 = 0.1484$	
6.16^{a}	0.926^{a}	6.78^{a}	0.905^{a}	7.34^{a}	0.884^{a}	7.96^{a}	0.862^{a}
6.76	0.931	7.28	0.909	7.82	0.889	8.31	0.866
7.26	0.936	7.78	0.914	8.27	0.894	8.77	0.872
7.73	0.939	8.29	0.918	8.78	0.899	9.25	0.877
8.25	0.943	8.76	0.922	9.30	0.904	9.76	0.883
8.78	0.947	9.25	0.926	9.80	0.908	10.28	0.888
9.26	0.950	9.77	0.930	10.27	0.912	10.74	0.893
9.74	0.953	10.24	0.934	10.72	0.916	11.23	0.897

Table 3. Continued

P/MPa	ρ/g·cm^{-3}	P/MPa	ρ/g·cm^{-3}	P/MPa	ρ/g·cm^{-3}	P/MPa	ρ/g·cm^{-3}
10.23	0.956	10.74	0.937	11.23	0.920	11.76	0.901
10.77	0.960	11.28	0.941	11.72	0.924	12.24	0.905
11.23	0.962	11.77	0.944	12.26	0.928	12.77	0.910
11.74	0.966	12.33	0.948	12.82	0.932	13.26	0.913
12.23	0.969	12.79	0.951	13.41	0.936	13.76	0.918
12.74	0.971	13.31	0.955	13.90	0.939	14.33	0.922
13.27	0.975	13.79	0.957	14.39	0.942	14.82	0.925
13.82	0.978	14.43	0.961	15.14	0.947	15.51	0.930
14.27	0.980	15.10	0.965	15.77	0.950	16.42	0.936
15.03	0.984	15.65	0.968	16.42	0.955		
15.69	0.987	16.47	0.972				
16.35	0.990						
T/K = 327.95		T/K = 332.85		T/K = 337.45			
$x_2 = 0.1484$		$x_2 = 0.1484$		$x_2 = 0.1484$			
8.54[a]	0.839[a]	9.18[a]	0.814[a]	9.76[a]	0.790[a]		
8.84	0.844	9.62	0.821	10.06	0.795		
9.29	0.850	9.92	0.826	10.53	0.804		
9.75	0.856	10.29	0.832	10.82	0.809		
10.24	0.862	10.72	0.839	11.23	0.816		
10.77	0.868	11.25	0.846	11.72	0.823		
11.26	0.873	11.73	0.851	12.24	0.830		
11.76	0.878	12.26	0.858	12.74	0.838		
12.26	0.883	12.75	0.863	13.24	0.843		
12.80	0.888	13.27	0.869	13.73	0.849		
13.31	0.893	13.80	0.874	14.27	0.855		
13.80	0.897	14.52	0.881	14.78	0.861		
14.24	0.901	15.02	0.885	15.35	0.866		
14.78	0.905	15.46	0.889	15.80	0.870		
15.30	0.909	15.94	0.893	16.60	0.881		
15.86	0.913	16.67	0.899				
16.56	0.918						

[a] Bubble point. [b] Critical point. [c] Dew point.

phase boundary data of the system were modeled using the Peng−Robinson equation of state (PR EoS) with two binary parameters.

Experimental Section

Materials. CO_2 with a mass fraction purity of 0.99995 was purchased from the Beijing Haipu Company. DMC (analytical reagent grade) was purchased from Alfa Aesar with a mass fraction purity of more than 0.995 as determined by gas chromatography.

Apparatus and Procedure. The phase behavior and the densities of the mixtures were determined using a high-pressure, variable-volume view cell, and the apparatus and procedures were similar to those used in the previous papers.[19,20] The volume of the view cell could be changed in the range from (23 to 50) cm^3 by moving the piston. The constant-temperature water bath was controlled by a temperature controller (A2, Beijing Changliu Scientific Instrument Co.), and the temperature was monitored by a Pt resistance thermometer with the accuracy of ± 0.1 K. The pressure gauge was composed of a pressure transducer and an indicator (Beijing Tianchen Instrument Co.). Its uncertainty was ± 0.025 MPa in the pressure range of (0 to 20) MPa.

In a typical experiment, a known mass of DMC was charged first using a syringe, and then the air in the system was flushed with CO_2. CO_2 was then added using the sample bomb. The mass of the chemicals in the system was calculated from the mass difference of the sample bomb before and after charging the system. The cell was placed into the water bath at the desired temperature. After thermal equilibration, the piston in the view cell was moved up and down to change the volume and the pressure of the system, and the phase separation could be observed directly. At the critical point, very strong opalescence was observed, and the meniscus appeared at half volume after a slight pressure reduction. The volume of the system was known from the position of the piston, which was calibrated accurately using water as a medium. The composition and density of the mixture could easily be calculated from the masses of the components and the volume of the system.

It is estimated that the uncertainty of the density data is ± 0.002 g·cm^{-3}, and the uncertainty in the compositions of samples is better than ± 0.5 %. To calculate the compressibility (K_T), we used a B-spline method to smooth the measured density data, and K_T was obtained by a differential calculation. It is estimated that the uncertainty of the K_T data is better than ± 3 %.

Correlation

The phase behaviors of CO_2-containing binary mixtures over wide ranges of temperatures and pressures have been correlated satisfactorily by PR EoS[21] with van der Waals mixing rules,[16,17,22−24] because the PR EoS requires comparatively little input information and many of the parameters (such as interaction parameters for mixtures) are always available in the literature for PR EoS. Therefore, in the present work, the PR EoS with the van der Waals mixing rules[21] was selected to correlate the phase behavior of the CO_2 + DMC binary mixtures.

The explicit form for this equation is expressed as follows.

$$P = \frac{RT}{v - b} - \frac{a}{v(v + b) + b(v - b)} \tag{1}$$

The constants a and b can be obtained from the related parameters of pure components. For a mixture, the van der Waals mixing rules are presented:

$$a = \sum_i \sum_j x_i x_j \sqrt{a_i a_j}(1 - k_{ij}) \tag{2}$$

$$b = \sum_i \sum_j 0.5 x_i x_j (b_i + b_j)(1 - l_{ij}) \tag{3}$$

where a_i and b_i are parameters of pure components, k_{ij} and l_{ij} are the binary parameters for the (i, j) pair, and x_i is the mole fraction of the ith component.

The physical property information (T_C, P_C, and ω) used for the pure components CO_2 and DMC is taken from the literature (see Table 1).

Binary parameters are empirical parameters that can be regressed from the binary data by minimizing the average absolute deviation for bubble and dew point pressures. The k_{ij} and l_{ij} values for these binary mixtures involved in this work are shown in Table 1; they were obtained by minimizing the following objective function (OF).

$$\mathrm{OF} = \frac{1}{n}\sum_{i=1}^{n}\left|\frac{\xi^{\mathrm{exptl}} - \xi^{\mathrm{calcd}}}{\xi^{\mathrm{exptl}}}\right| \tag{4}$$

where n is the number of experimental points and ξ^{exptl} and ξ^{calcd} are the experimental and the calculated pressure at each phase transition point, respectively.

The average absolute relative deviation (AARD) of this calculation was defined as follows:

$$\mathrm{AARD} = \frac{1}{n}\sum_{i=1}^{n}\left|\frac{\xi^{\mathrm{exptl}} - \xi^{\mathrm{calcd}}}{\xi^{\mathrm{exptl}}}\right| \times 100\ \% \tag{5}$$

The corresponding values of AARD are also shown in Table 1.

Results and Discussion

Critical Points and Phase Behavior of the Mixtures. First, to verify the reliability of the apparatus, our results are compared

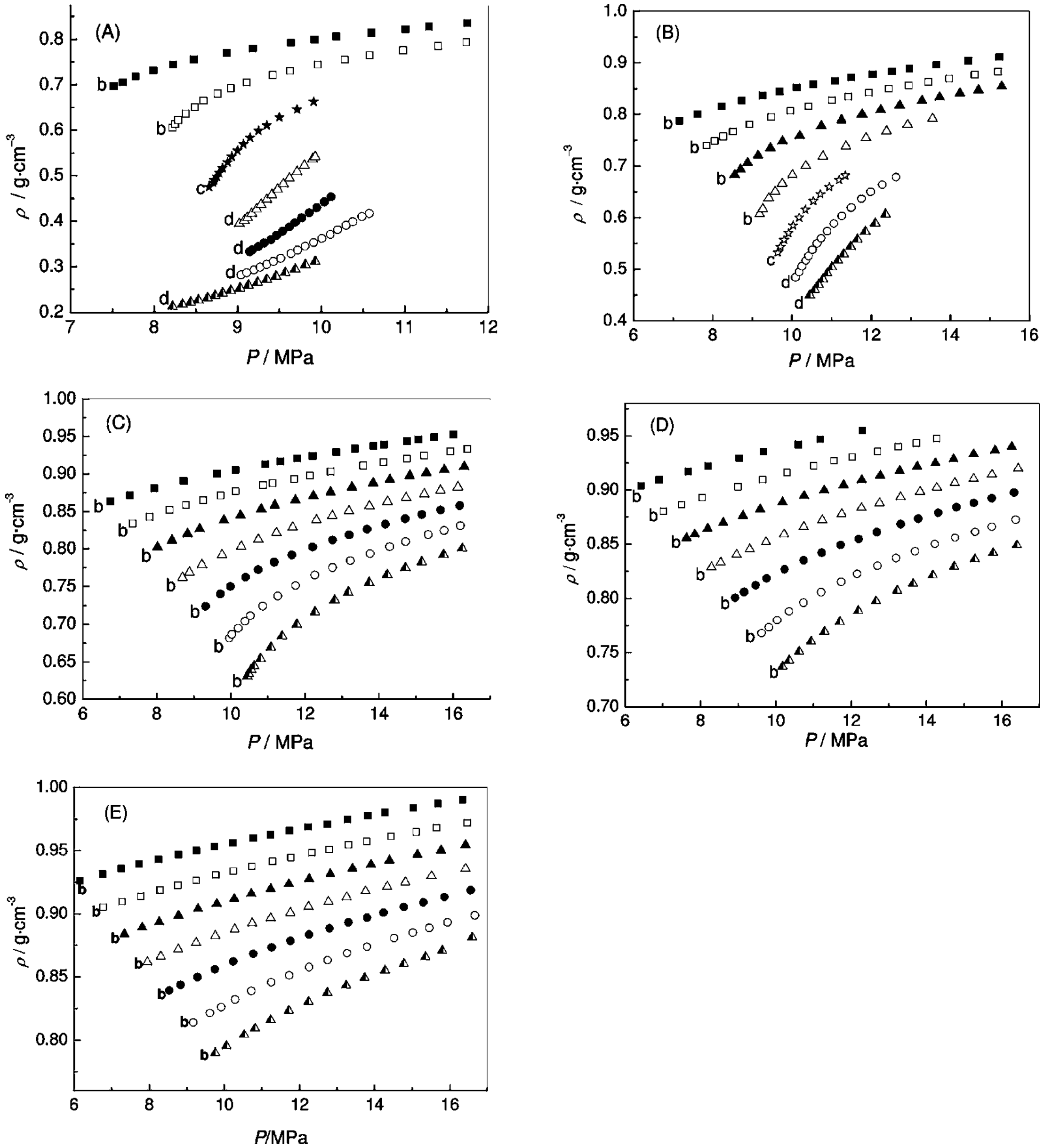

Figure 3. Dependence of the density of the CO_2 (1) + DMC (2) binary mixture on temperature and pressure in the critical region with different compositions: (A) $x_2 = 0.0242$; (B) $x_2 = 0.0481$; (C) $x_2 = 0.0860$; (D) $x_2 = 0.1180$; (E) $x_2 = 0.1484$. Temperatures are labeled as follows: ■, $T = 308.15$ K; □, $T = 313.15$ K; ★, $T = 317.85$ K; ▲, $T = 318.15$ K; △, $T = 323.15$ K; ●, $T = 327.95$ K; ☆, 328.15 K; ○, $T = 332.85$ K; ◭, $T = 337.45$ K. b, bubble point; d, dew point; c, critical point.

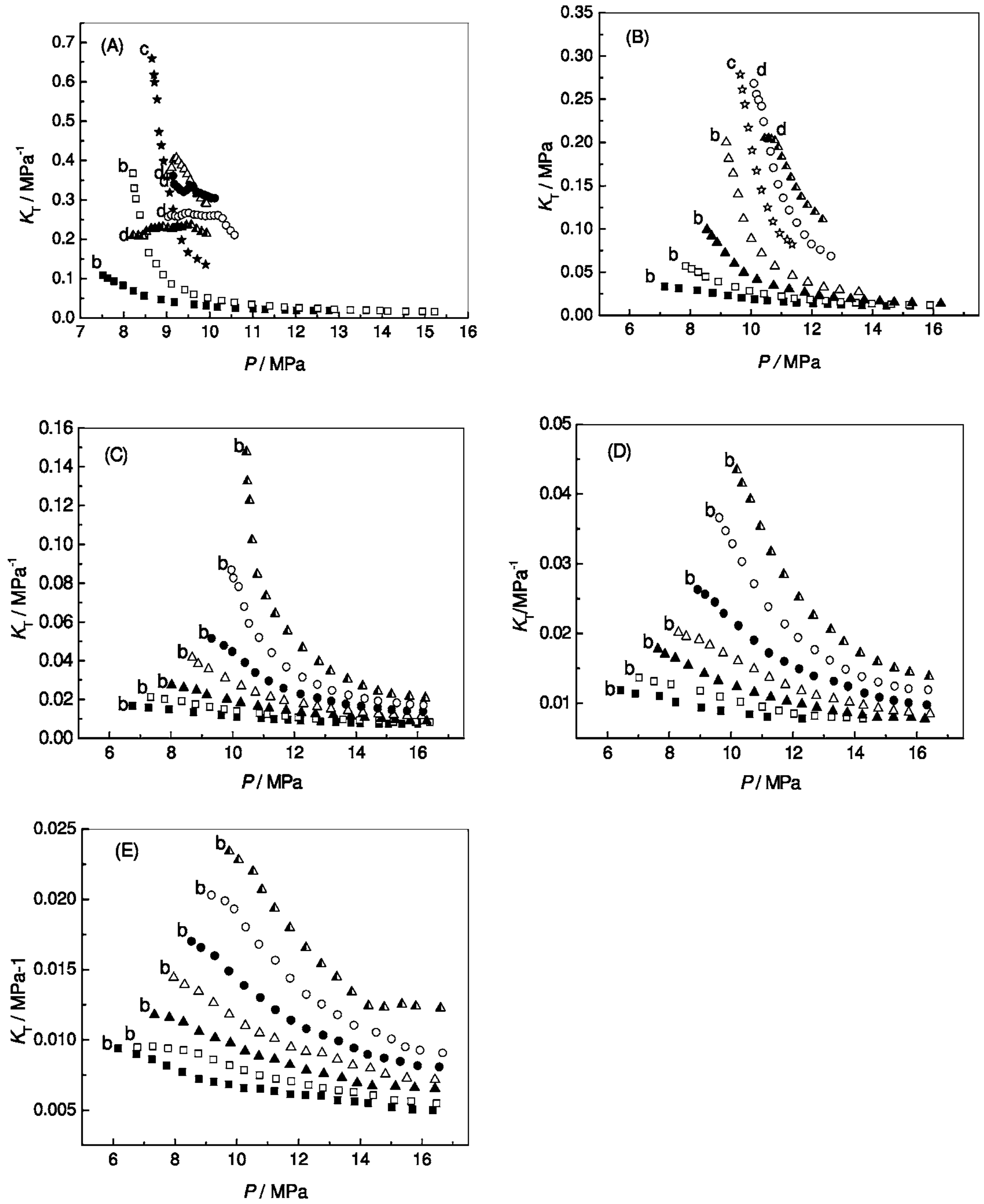

Figure 4. Dependence of the isothermal compressibility (K_T) of the CO_2 (1) + DMC (2) binary mixture on temperature and pressure with different compositions: (A) $x_2 = 0.0242$; (B) $x_2 = 0.0481$; (C) $x_2 = 0.0860$; (D) $x_2 = 0.1180$; (E) $x_2 = 0.1484$. Temperatures are labeled as follows: ■, $T = 308.15$ K; □, $T = 313.15$ K; ★, $T = 317.85$ K; ▲, $T = 318.15$ K; △, $T = 323.15$ K; ●, $T = 327.95$ K; ☆, 328.15 K; ○, $T = 332.85$ K; ◭, $T = 337.45$ K. b, bubble point; d, dew point; c, critical point.

with the data reported by Camy et al.,[15] which is shown in Figure 1. The figure indicates that our results about CO_2 + DMC are in a good agreement with the literature.

Table 2 summarizes the bubble point, critical point, and dew point temperatures and pressures for the binary system with DMC concentrations from (0.0242 to 0.1484) mole fraction. The critical point is located between the bubble point and the dew point if there is no critical point shown at the composition. Figure 2 gives a graphical representation of the experimentally determined phase boundaries. There is a two-phase region below or inside lines of fixed composition, while the one phase region is above or outside of these lines.

Density and Isothermal Compressibility. The densities of the mixture at temperatures from (308.15 to 337.45) K and at pressures from (6.16 to 16.67) MPa were measured using the high-pressure, variable-volume view cell. The data determined at different conditions are listed in Table 3. Figure 3 illustrates the dependence of the density of the binary mixtures on pressure and temperature. It can be seen from Figure 3 that the similar tendency was observed for different compositions. Obviously, at fixed composition and fixed temperature, the density increases with increasing pressure, and at fixed composition and fixed pressure, the density decreases with increasing temperature. When the concentration of DMC increases, the density also increases, which reason is probably that the molecular weight of DMC is greater than that of CO_2.

As pressures approach the phase boundary, especially near the critical point, the density of the mixture changes greatly.

For example, when the concentration of DMC is 0.0242 mole fraction, the critical temperature is 317.85 K, and critical pressure is 8.66 MPa. The density of the mixture decreases greatly when the pressure decreases to the critical point. However, when the pressure is far away from the phase boundary, the density has no obvious change.

The results in Figure 3 demonstrate that the sensitivity of density to pressure depends on both the composition and the pressure at a fixed temperature. The isothermal compressibility (K_T) of a fluid is a quantitative expression of the sensitivity of density to pressure, which is closely related with the structure of fluids. K_T values of the mixture can be calculated by the following equation:

$$K_T = \frac{1}{\rho}\left(\frac{\partial \rho}{\partial P}\right)_T \tag{6}$$

where ρ is the density of fluid and P is the pressure.

Figure 4 shows the effect of the pressure on K_T for mixtures of different compositions. As can be seen from the figures, K_T is large and sensitive to the pressure as the pressure approaches the critical point of a mixture; that is, K_T increases sharply as the pressure approaches the critical pressure. It also can be seen that K_T increases significantly as the pressure approaches the values at the dew and bubble points. However, K_T is very small and not sensitive to the pressure when the pressure is far away from the phase separation pressure.

The data in Figure 4 also illustrate that, when the temperature is far from the critical temperature, the effect of pressure on K_T is limited, even near the phase separation point, especially in the Figures 4D,E.

Modeling. For modeling the phase behavior of the CO_2 and DMC binary system using PR EoS, the two binary parameters need to be regressed from the experimental data. The two binary parameters regressed are shown in Table 1.

On the basis of the physical properties and the two binary parameters, the PR EoS was used to correlate the phase behavior of the CO_2 + DMC binary mixture. The correlation results are also shown in Figure 2 (see lines). It can be seen from the figure that the PR EoS can correlate the phase boundary of three binary systems to a satisfactory degree at DMC concentrations from (0.0242 to 0.1484) mole fraction with AARD = 2.3 %.

Conclusions

The phase behavior and densities for the system CO_2 + DMC were measured at pressures from (2.76 to 12.83) MPa with concentrations from (0.0242 to 0.1484) of DMC mole fraction. The effect of pressure on the density, ρ, and isothermal compressibility, K_T, has been studied, and these properties are sensitive to the pressure approaching phase transition points, especially close to the critical points. The PR EoS with two binary parameters can correlate the binary phase behavior to a satisfied degree.

Acknowledgment

We thank Prof. C. Li, Prof. Z. Liu, and Dr. Q. Liu for their help.

Literature Cited

(1) Tundo, P.; Selva, M. The Chemistry of Dimethyl Carbonate. *Acc. Chem. Res.* **2002**, *35*, 706–716.

(2) Tundo, P.; Memoli, S.; Hérault, D.; Hill, K. Synthesis of Methylethers by Reaction of Alcohols with Dimethyl Carbonate. *Green Chem.* **2004**, *6*, 609–612.

(3) Tundo, P.; Selva, M.; Perosa, A.; Memoli, S. Selective Mono-*C*-methylations of Arylacetonitriles and Arylacetates with Dimethylcarbonate: A Mechanistic Investigation. *J. Org. Chem.* **2002**, *67*, 1071–1077.

(4) Pacheco, M. A.; Marshall, C. L. Review of Dimethyl Carbonate (DMC) Manufacture and Its Characteristics as a Fuel Additive. *Energy Fuels* **1997**, *11*, 2–29.

(5) Delledonne, D.; Rivetti, F.; Romano, U. Developments in the Production and Application of Dimethyl Carbonate. *Appl. Catal., A* **2001**, *221*, 241–251.

(6) Ballivet-Tkatchenko, D.; Chambrey, S.; Keiski, R.; Ligabue, R.; Plasseraud, L.; Richard, P.; Turunen, H. Direct Synthesis of Dimethyl Carbonate with Supercritical Carbon Dioxide: Characterization of a Key Organotin Oxide Intermediate. *Catal. Today* **2006**, *115*, 80–87.

(7) Bian, J.; Xiao, M.; Wang, S.; Wang, X.; Lu, Y.; Meng, Y. Highly Effective Synthesis of Dimethyl Carbonate from Methanol and Carbon Dioxide Using a Novel Copper-Nickel/Graphite Bimetallic Nanocomposite Catalyst. *Chem. Eng. J. (Amsterdam, Neth.)* **2009**, *147*, 287–296.

(8) Yoshida, Y.; Arai, Y.; Kado, S.; Kunimori, K.; Tomishige, K. Direct Synthesis of Organic Carbonates from the Reaction of CO_2 with Methanol and Ethanol over CeO_2 Catalysts. *Catal. Today* **2006**, *115*, 95–101.

(9) Wu, X. L.; Xiao, M.; Meng, Y. Z.; Lu, Y. X. Direct Synthesis of Dimethyl Carbonate on H_3PO_4 Modified V_2O_5. *J. Mol. Catal. A: Chem.* **2005**, *238*, 158–162.

(10) Brennecke, J. F.; Chateauneuf, J. E. Homogeneous Organic Reactions as Mechanistic Probes in Supercritical Fluids. *Chem. Rev.* **1999**, *99*, 433–452.

(11) Pereda, S.; Bottini, S. B.; Brignole, E. A. Supercritical Fluids and Phase Behavior in Heterogeneous Gas-Liquid Catalytic Reactions. *Appl. Catal., A* **2005**, *281*, 129–137.

(12) Chouchi, D.; Gourgouillon, D.; Courel, M.; Vital, J.; Nunes da Ponte, M. The Influence of Phase Behavior on Reactions at Supercritical Conditions: The Hydrogenation of α-Pinene. *Ind. Eng. Chem. Res.* **2001**, *40*, 2551–2554.

(13) Hou, Z. S.; Han, B. X.; Liu, Z. M.; Jiang, T.; Yang, G. Y. Synthesis of Dimethyl Carbonate Using CO_2 and Methanol: Enhancing the Conversion by Controlling the Phase Behavior. *Green Chem.* **2002**, *4*, 467–471.

(14) Piñero, R.; García, J.; Sokolova, M.; Cocero, M. J. Modelling of the Phase Behaviour for the Direct Synthesis of Dimethyl Carbonate from CO_2 and Methanol at Supercritical or near Critical Conditions. *J. Chem. Thermodyn.* **2007**, *39*, 536–549.

(15) Camy, S.; Pic, J.-S.; Badens, E.; Condoret, J.-S. Fluid Phase Equilibria of the Reacting Mixture in the Dimethyl Carbonate Synthesis from Supercritical CO_2. *J. Supercrit. Fluids* **2003**, *25*, 19–32.

(16) Im, J.; Kim, M.; Lee, J.; Kim, H. Vapor-Liquid Equilibria of Binary Carbon Dioxide + Alkyl Carbonate Mixture Systems. *J. Chem. Eng. Data* **2004**, *49*, 243–245.

(17) Lu, C.; Tian, Y.; Xu, W.; Li, D.; Zhu, R. High-Pressure Phase Equilibrium for the Binary Systems of {Carbon Dioxide (1) + Dimethyl Carbonate (2)} and {Carbon Dioxide (1) + Diethyl Carbonate (2)} at Temperatures of 273 K, 283 K, and 293 K. *J. Chem. Thermodyn.* **2008**, *40*, 321–329.

(18) Guo, X. C.; Qin, Z. F.; Wang, G. F.; Wang, J. G. Critical Temperatures and Pressures of Reacting Mixture in Synthesis of Dimethyl Carbonate with Methanol and Carbon Dioxide. *Chin. Chem. Let.* **2008**, *19*, 249–252.

(19) Chen, J. W.; Wu, W. Z.; Han, B. X.; Gao, L.; Mu, T. C.; Liu, Z. M.; Jiang, T.; Du, J. M. Phase Behavior, Densities, and Isothermal Compressibility of CO_2 + Pentane and CO_2 + Acetone Systems in Various Phase Regions. *J. Chem. Eng. Data* **2003**, *48*, 1544–1548.

(20) Hou, Y. C.; Wu, W. Z.; Poliakoff, M. The Phase Behavior, Densities, and Isothermal Compressibility of CO_2 + γ-valerolactone Systems in Various Phase Regions. *J. Chem. Eng. Data* **2009**, *54*, 118–126.

(21) Peng, D. Y.; Robinson, D. B. A New Two-Constant Equation of State. *Ind. Eng. Chem. Res.* **1976**, *15*, 59–64.

(22) Ndiaye, P. M.; Franceschi, E.; Oliveira, D.; Dariva, C.; Tavares, F. W.; Vladimir Oliveira, J. Phase Behavior of Soybean Oil, Castor Oil and Their Fatty Acid Ethyl Esters in Carbon Dioxide at High Pressures. *J. Supercrit. Fluids* **2006**, *37*, 29–37.

(23) Lazzaroni, M. J.; Bush, D.; Brown, J. S.; Eckert, C. A. High-Pressure Vapor-Liquid Equilbria of Some Carbon Dioxide + Organic Binary Systems. *J. Chem. Eng. Data* **2005**, *50*, 60–65.

(24) Schwinghammer, S.; Siebenhofer, M.; Marr, R. Determination and Modelling of the High-Pressure Vapour-Liquid Equilibrium Carbon Dioxide-Methyl Acetate. *J. Supercrit. Fluids* **2006**, *38*, 1–6.

(25) Poling, B.; Prausnitz, J.; O'Connel, J. *The Properties of Gases and Liquids*, 5th ed.; McGraw-Hill: New York, 2001.

Received for review August 20, 2009. Accepted September 16, 2009. This work was supported by the National Natural Science Foundation of China (20776004), Beijing Natural Science Foundation (2082017), and Program for New Century Excellent Talents in University.

JE900691N